



# Temporal and spatial evolution of bottom-water hypoxia in the Estuary and Gulf of St. Lawrence

Mathilde Jutras<sup>1,4</sup>, Alfonso Mucci<sup>1,5</sup>, Gwenaëlle Chaillou<sup>2,4</sup>, William A. Nesbitt<sup>3</sup> and Douglas W.R. Wallace<sup>3</sup>

<sup>1</sup>Department of Earth and Planetary Sciences, McGill University, 3450 University Street, Montreal, QC, H3A OE8, Canada

<sup>2</sup>Institut des Sciences de la Mer de Rimouski (ISMER) - Université du Québec à Rimouski, 300 Allée des Ursulines, Rimouski, QC, G5L 3A1, Canada

10 <sup>3</sup>Department of Oceanography, Dalhousie University, Steele Ocean Sciences Building, 1355 Oxford St., PO Box 15000, Halifax, NS, B3H 4R2, Canada

<sup>4</sup>Québec-Océan

<sup>5</sup>GEOTOP

*Correspondence to:* Mathilde Jutras (mathilde.jutras@mail.mcgill.ca)

15 **Abstract.** Persistent hypoxic bottom waters have developed in the Lower St. Lawrence Estuary (LSLE) and have impacted fish and benthic species distributions. Minimum dissolved oxygen concentrations decreased from  $\sim 125 \mu\text{mol L}^{-1}$  (38% saturation) in the 1930s to  $\sim 65 \mu\text{mol L}^{-1}$  (21% saturation) in 1984. Dissolved oxygen concentrations remained at hypoxic levels ( $< 62.5 \mu\text{M} = 2 \text{ mg l}^{-1}$  or 20% saturation) between 1984 and 2019 but, in 2020, they suddenly decreased to  $\sim 35 \mu\text{mol L}^{-1}$ . Concurrently, bottom-water temperatures in the LSLE have increased progressively from  $\sim 3^\circ\text{C}$  in the 1930's to nearly  
20  $7^\circ\text{C}$  in 2021. The main driver of deoxygenation and warming in the bottom waters of Gulf and St. Lawrence Estuary is a change in the circulation pattern in the western North Atlantic, more specifically a decrease in the relative contribution of younger, well-oxygenated and cold Labrador Current Waters to the waters of the Laurentian Channel, a deep valley that extends from the continental shelf edge, through Cabot Strait, the Gulf and to the head of the LSLE. Hence, the warmer, oxygen-depleted North Atlantic Central Waters carried by the Gulf Stream now make up nearly 100% of the waters entering  
25 the Laurentian Channel. The areal extent of the hypoxic zone in the LSLE has varied since 1993 when it was first estimated at  $1300 \text{ km}^2$ . In 2021, it reached  $9700 \text{ km}^2$ , extending well into the western Gulf of St. Lawrence. Severely hypoxic waters are now also found at the end of the two deep channels that branch out from the Laurentian Channel, namely the Esquiman and Anticosti Channels.

## 1 Introduction

30 Hypoxia and anoxia occur naturally in many coastal environments with restricted circulation, such as fjords and embayments (e.g., Saanich Inlet in British Columbia, Bedford Basin in Nova Scotia, Chesapeake Bay in Maryland), inland seas (e.g., Baltic Sea), but hypoxia in more open coastal and estuarine areas appears to be on the rise due to anthropogenic



35 nutrient loading and coastal eutrophication (e.g. shelf region of the northern Gulf of Mexico, the Kattegat, the Bengali Current in western Africa, and the coastal area of the Changjian River/Estuary in the East China Sea) (Bindoff et al., 2019; Breitburg et al., 2018; Gilbert et al., 2010; Rabalais et al., 2010; Li et al., 2002). Where the water column is shallow or seasonally stratified, such areas are not hypoxic throughout the year; they are ventilated seasonally through fall and winter mixing events (e.g., Gulf of Mexico).

40 Persistent hypoxia in coastal and estuarine environments is less common but has been identified at a number of locations where the water column is permanently and strongly stratified, including the Lower St. Lawrence Estuary in Eastern Canada (Genovesi et al., 2011; Thibodeau et al., 2006; Gilbert et al., 2005). Gilbert et al. (2005) first reported the presence of severely hypoxic bottom waters ( $[O_2] < 62.5 \mu\text{M} = 2 \text{ mg l}^{-1}$  or 20% saturation) in the Lower St. Lawrence Estuary (LSLE). In 2003, the hypoxic zone in the LSLE covered an estimated 1300 km<sup>2</sup>.

45 Oxygen depletion in the bottom waters of the LSLE and the development of persistent hypoxic levels has had a direct impact on marine fauna and fisheries, including fish growth and distribution (Brown-Vuillemin et al., 2022; Dupont-Prinet et al., 2013; Petersen 2010; Chabot and Claireaux, 2008; Chabot and Dutil, 1999; D'Amours, 1993) and northern shrimp viability (Dupont-Prinet et al., 2013). At hypoxic levels, the benthic community structure is believed to undergo significant modifications (Riedel et al., 1997; Levin, 2003; Belley et al., 2010; Audet et al., 2022) while catabolic reactions and diagenetic cycling of redox-sensitive elements in the sediments are altered (Riedel et al., 1999; Katsev et al., 2007; Lefort et al., 2012).

## 50 1.1 The St. Lawrence Estuary

By most definitions, the Gulf and St. Lawrence Estuary make up the largest estuarine system on Earth (Figure 1). The greater St. Lawrence System connects the Great Lakes to the Atlantic Ocean. With a drainage basin of approximately 1.32 million km<sup>2</sup>, the St. Lawrence River channels the second largest freshwater discharge ( $\sim 12,000 \text{ m}^3 \text{ s}^{-1}$ ) on the North American continent, second only to that of the Mississippi. The St. Lawrence Estuary (SLE) begins at the landward limit of the salt-water intrusion at the eastern tip of Île d'Orléans (5 km downstream of Québec City) and stretches 400 km seaward to Pointe-des-Monts where it widens into the Gulf of St. Lawrence (GSL). Traditionally, the SLE is divided into two segments based on its bathymetry and hydrographic features. The Upper St. Lawrence Estuary (USLE), extends from Île d'Orléans to Tadoussac, near the mouth of the Saguenay Fjord. This segment is relatively narrow (2 to 24 km wide) and mostly shallow, with depths typically under 30 m. Consequently, while it displays strong lateral salinity gradients, the water column is only weakly stratified. In contrast, the LSLE is much larger, wider (30 to 50 km) and deeper ( $\sim 300 \text{ m}$ ), displays a smoother, less variable bottom topography, and is more strongly stratified.

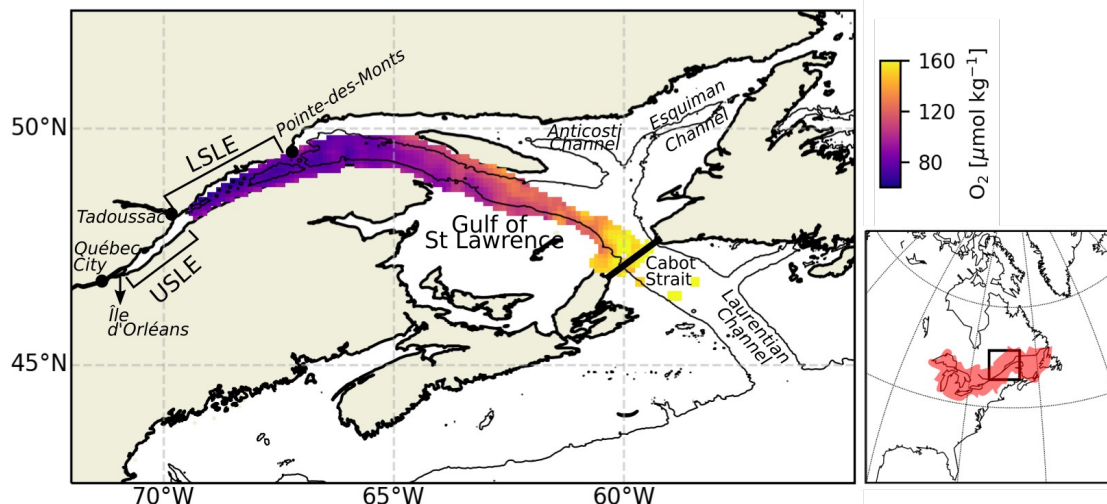


**Figure 1:** Map of the LSLE, including the mean bottom-water oxygen concentration between 1970 and 2018. The thin black line delineates the 250 m isobath. The map on the right shows the drainage basin of the LSLE.

65

The dominant bathymetric feature of the Lower Estuary and Gulf is the Laurentian Channel (or Trough), a deep U-shaped valley that extends 1280 km from the eastern Canadian continental shelf break through the GSL and into the LSLE. From this channel, two other deep channels branch out to the northeast within the gulf: the Esquiman and the Anticosti Channels (Figure 1). During most of the ice-free season, the water column of the LSLE can be described as a three-layer system on the basis of its thermal stratification. A warm and relatively fresh surface layer (0 to 30 m) that flows seaward overlies the cold intermediate layer (CIL, 30-150 m deep;  $S_p = 32.0$  to  $32.6$ , where  $S_p$  stands for practical salinity) that flows landward and is formed in the wintertime in the GSL (Galbraith, 2006). Below the CIL, a warmer (2 to 7°C) and saltier ( $S_p = 33$  to  $35$ ) bottom layer (>150 m deep) flows sluggishly landward (Dickie & Trites, 1983) in 4 to 7 years from the continental shelf-break to the head of the Laurentian Channel (Bugden et al., 1991; Gilbert, 2004). There, complex tidal phenomena due to rapid shoaling (tidal movements, including internal tides and strong flows over the steep sill) generate significant local mixing of near-surface waters with deep nutrient-rich saline waters (Jutras et al., 2020a; Cyr et al., 2015; Saucier & Chassé, 2000; Ingram, 1983), resulting in a fertile surface layer that sustains a feeding habitat for several large marine mammals.

70

75

In this paper we provide an update on hypoxic conditions in the LSLE and GSL since our last report (Jutras et al., 2020b), given the observed, sudden drop in oxygen concentrations observed since then, and estimate the temporal evolution of the areal extent of the hypoxic zone since our first report (Gilbert et al., 2005).

80

## 2 Method

We use in situ observations throughout the water column from two data sets. The first data set includes measurements we acquired at various periods of the year, but mostly during the spring and summer, between 2003 and 2021, at multiple stations (Figure 2) along the Laurentian Channel, onboard the RV Alcide C. Horth, the RV Coriolis II and the CCGS Amundsen. In all cases, sampling of the water column was carried out with a rosette system (12 or 24 x 12-L Niskin bottles) equipped with a Seabird 911Plus conductivity-temperature-depth (CTD) probe, a Seabird® SEB-43 oxygen probe and a Seapoint® fluorometer. The Niskin bottles were closed at discrete depths as the rosette was raised from the bottom,

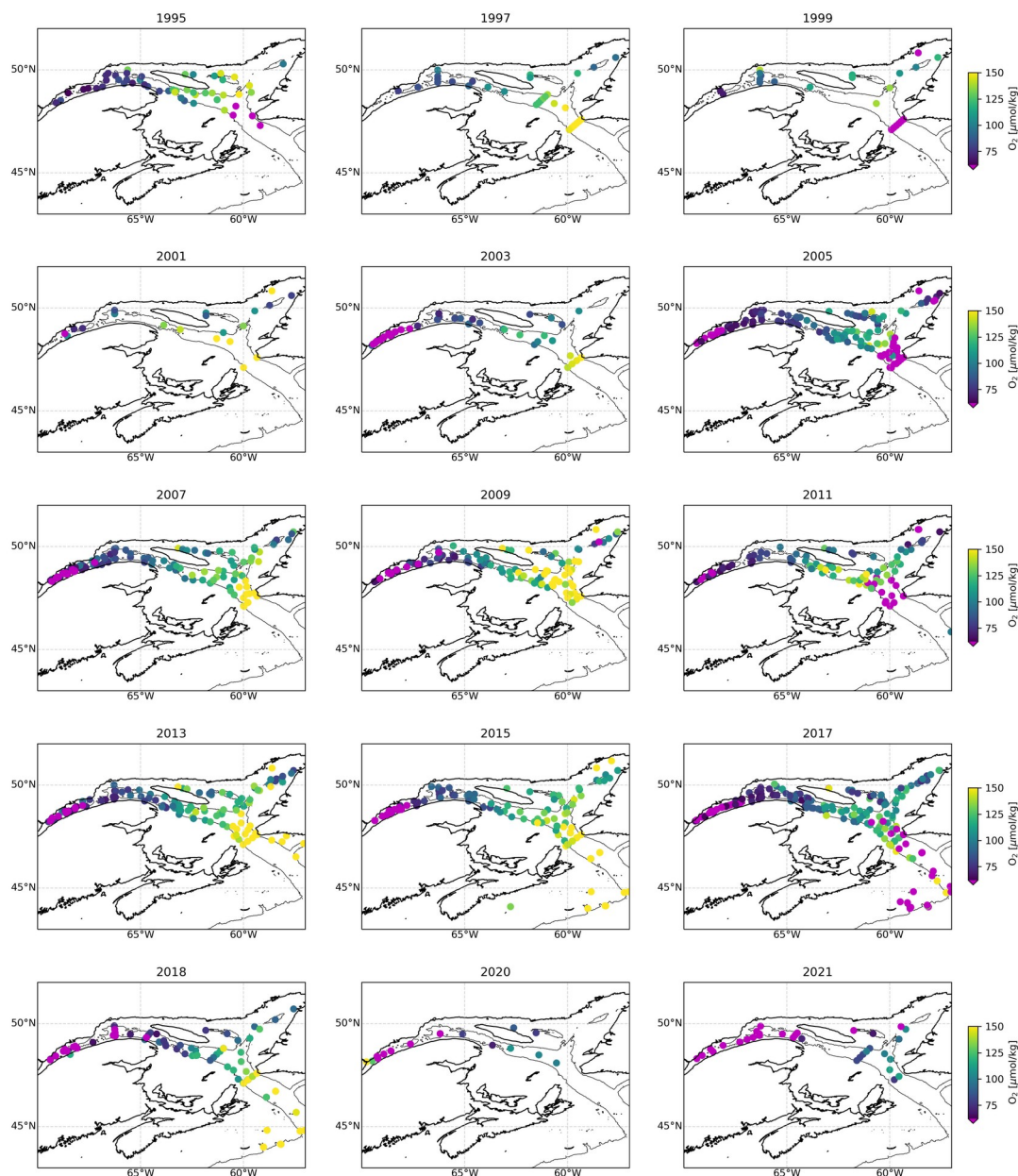
85



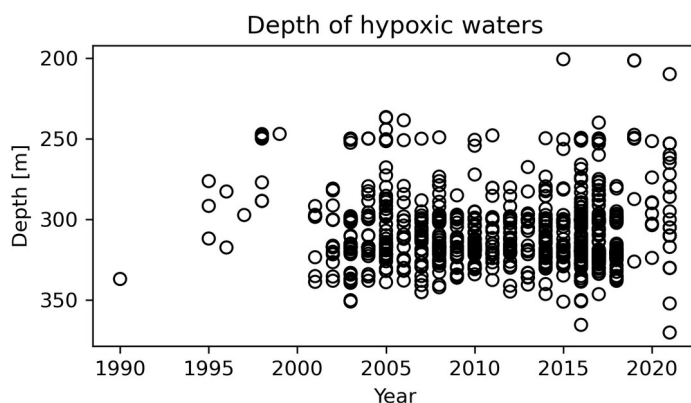
typically at the surface (2-3m), 25m, 50m, 75m, 100m, and at 50m intervals to the bottom (or within 10m of the bottom). Even though the probes had been calibrated by the manufacturer within the year, discrete salinity samples were collected throughout the water column and analyzed on a Guildline Autosal 8400 salinometer calibrated with IAPSO standard seawater and CTD profiles reprocessed post-cruise. Likewise, dissolved oxygen concentrations were determined by Winkler titration (Grasshoff et al., 1999) on distinct water samples recovered directly from the Niskin bottles. The relative standard deviation, based on replicate analyses of samples recovered from the same Niskin bottle, was better than 1 %. These measurements further served to calibrate the SBE-43 oxygen probe mounted on the rosette. The second data set was extracted from the Bio-Chem database compiled by the Department of Fisheries and Oceans Canada. This data set provides quality-controlled data for the same variables as described above, and covers the Gulf and St. Lawrence Estuary from 1967 to 1972, and from 1991 to 2018 (Devine et al., 2014; DFO, 2019). A detailed description of data sampling techniques and quality control can be found in Devine et al. (2014) and Mitchell et al. (2002). Oxygen saturation levels are calculated from temperature, salinity and oxygen concentrations using the Python seawater package ([pypi.org/project/seawater/](http://pypi.org/project/seawater/)).

We reconstruct the causes of the 2018 to 2021 deoxygenation by applying an extended Optimum-Multiparameter (eOMP) analysis on the combined dataset (Karstensen and Tomczak, 1998; Tomczak and Large, 1989; Tomczak, 1981). This method provides the proportion of the different water types composing a given water sample. Unlike the T-S diagram method, the eOMP accounts also provides estimates of biogeochemical changes that occurred between the water type formation and the measurement locations. Details of the application of this method to the current dataset can be found in Jutras et al. (2020b).

The spatial extent of the hypoxic zone is estimated from dissolved oxygen maps (Figure 2), by computing the area included within the 275 m isobath from the head of the LSLE to the downstream-most measurement location displaying hypoxic dissolved oxygen concentrations. The 275 m isobath is chosen because it is representative of the shallowest depth reached by the hypoxic waters (Figure 3). We use the General Bathymetric Chart of the Oceans (GEBCO) gridded bathymetry product with a 15 arc-second resolution. The uncertainty on the areal estimate is equal to the area between the seaward-most hypoxic station and the first non-hypoxic station. The area of hypoxic zones that are now observed at the head of the Esquiman and Anticosti Channels is not included in the calculation, given the large uncertainties at these locations due to lower data availability.



115 **Figure 2: Maps of bottom oxygen concentrations at each sampled station, for nearly every year since 1995. Hypoxic waters are represented in magenta. The thin black lines delineates the 275 m isobath.**



120 **Figure 3: Depth of hypoxic waters, through time. Each point represents one field observation of hypoxic waters (dissolved oxygen < 62.5 μM) within the LSLE.**

### 3 Results and discussion

#### 3.1 Historical reconstruction

125 An historical reconstruction of published and unpublished field data clearly reveals that oxygen depletion in the bottom waters of the LSLE is a persistent feature of the system and is evolving in time (Figure 4 and 5, Jutras et al., 2020b; Gilbert et al., 2005). The time series of bottom-water dissolved oxygen shows that, despite substantial inter-annual variability, three distinct clusters of points indicate that the range of yearly-averaged bottom-water dissolved oxygen decreased from 110-135 μM in the 1930s to 95-120 μM in the early 1970s and then to 55-65 μM in the 1990s. A linear least squares fit applied to the dissolved oxygen time series between 1930 and 1985 yields a decreasing trend of about  $-1.0 \pm 0.2$  μM/year at the 95% confidence level. The situation seemed to have stabilized after the mid-1980s as the trend in dissolved oxygen concentrations over the 1984-2016 period is not different from zero ( $-0.02 \pm 0.79$  μM/year at the 95% confidence level). In 2020, minimum dissolved oxygen concentrations suddenly decreased alarmingly fast. Minimum oxygen levels were nearly cut by half within one year, reaching concentrations of ~35 μM, compared to 55-60 μM since early 2000s. Concurrently, bottom-water temperatures in the LSLE and the GSL have increased progressively from ~3°C in the 1930's to nearly 7°C in 2021 (Figure 4). These levels are unprecedented in the recent history of the LSLE and the GSL, and impart an  
130  
135 extremely high stress on marine life and the health of this ecosystem.



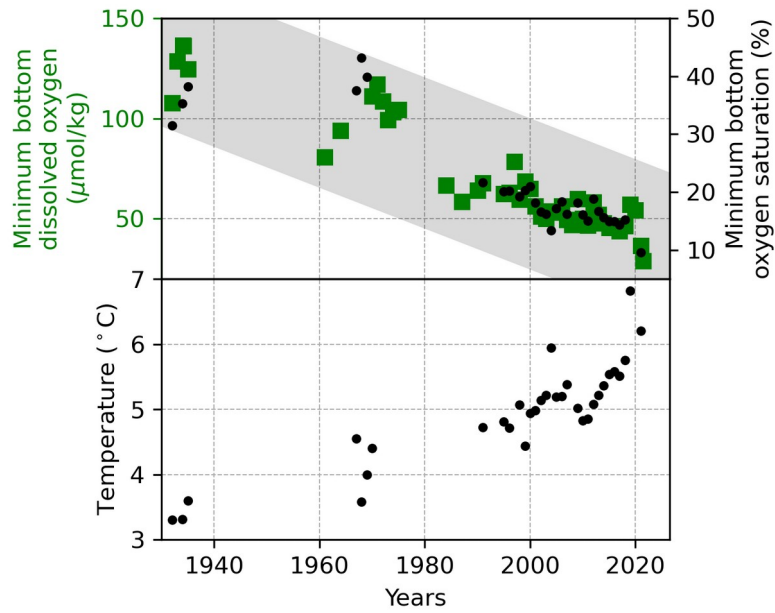


**Figure 4: Minimum bottom water dissolved oxygen concentration at the head of the LSLE (top), and associated water temperature (bottom).**

140

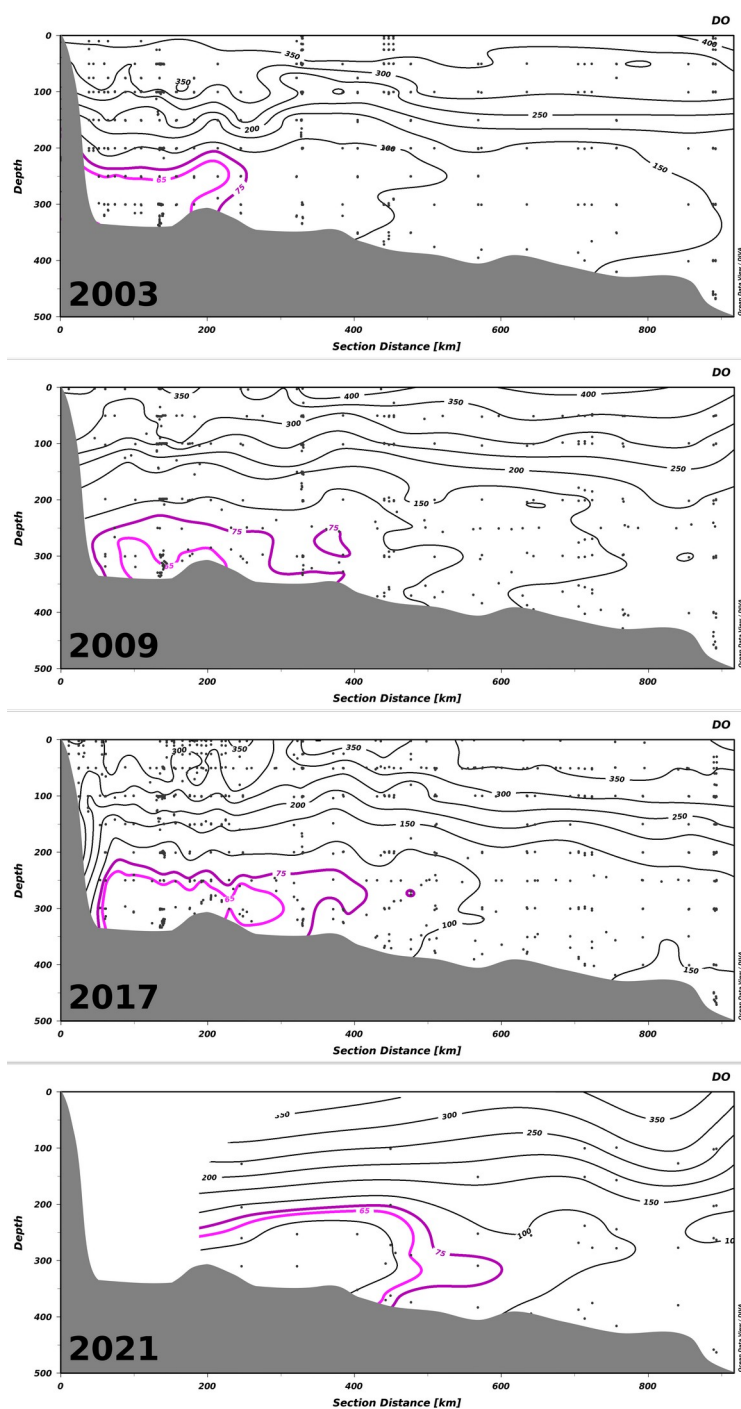


Figure 5: Transects of oxygen concentrations along the Laurentian Channel in 2003, 2009, 2017 and 2021, from the head of the channel (left) to Cabot Strait (right). Black dots indicate the location of measurements. Contours show oxygen concentrations, in  $\mu\text{M}$ . The hypoxic waters are delineated with the magenta contour. Zones with no data are left blank.

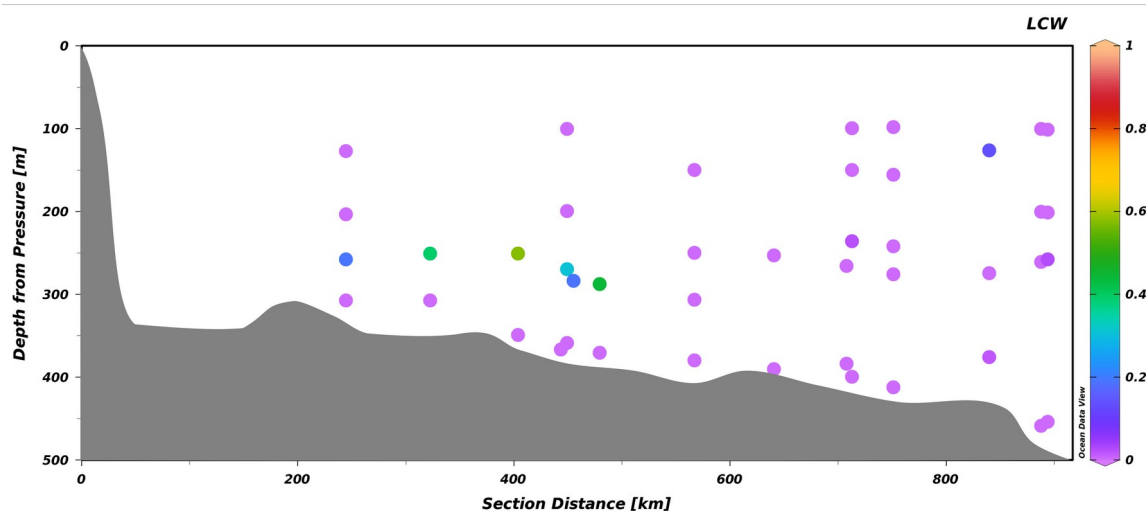




### 3.2 Causes

145 Several factors or combination of factors are responsible for the decrease in bottom water dissolved oxygen in the  
150 LSLE. Being isolated from the atmosphere, the bottom waters of the GSL and LSLE lose oxygen gradually through  
respiration and remineralization of organic matter as they flow landward (Figure 1). At depths greater than 150 m, the  
oxygen lost through microbial respiration in the water column and sediments cannot be replenished by winter convection,  
only by weak diffusion from the overlying water or by tidal mixing at the head of the Laurentian Channel (Cyr et al., 2015).  
For this reason, the oxygen balance is precarious: increased respiration and/or decreased deep estuarine landward flow speed  
will lead to lower oxygen concentrations. Unfortunately, there are few measurements of the mean flow of the bottom waters,  
but an analysis of the temperature field between 200 and 300 m depth along the Laurentian Channel reveals that the mean  
lateral flow may have increased slightly between two consecutive 26-year periods (1952-1977 and 1978-2003), in  
contradiction to the field observations, should have resulted in an increase of the dissolved oxygen concentrations (Gilbert et  
al., 2004).

155 An analysis of the physical and biogeochemical properties of the deep waters of the LSLE since the early 1930s  
revealed that a change in water circulation in the western North Atlantic, more specifically the relative contributions of the  
two parent water masses (Labrador Current and North Central Atlantic Waters) that mix on the continental shelf or slope and  
enter the Gulf of St. Lawrence (GSL) at depth through Cabot Strait, is responsible for most of the observed dissolved oxygen  
depletion and temperature increase (Jutras et al., 2020b; Gilbert et al., 2005). The remainder was attributed to eutrophication  
(Jutras et al., 2020b; Thibodeau et al., 2006) and an increase of microbial respiration rates of settling organic matter in  
160 response to the increase in bottom-water temperatures (Genovesi et al., 2010). The former is fostered by an increase in  
organic matter and nutrient exports from the estuary's main tributary, the St. Lawrence River (Environment and Climate  
Change Canada, 2018; Goyette et al., 2016). It drains a  $1.32 \times 10^6$  km<sup>2</sup> basin that includes highly populated (>45 million  
Canadians and Americans; ECCC, 2018) and industrialized areas, as well as intensively farmed and forested lands (Hudon et  
al., 2017).



165

Figure 6: Transect of the LCW fraction along the Laurentian Channel in 2021, from the head of the Laurentian Channel (left) to Cabot Strait (right).

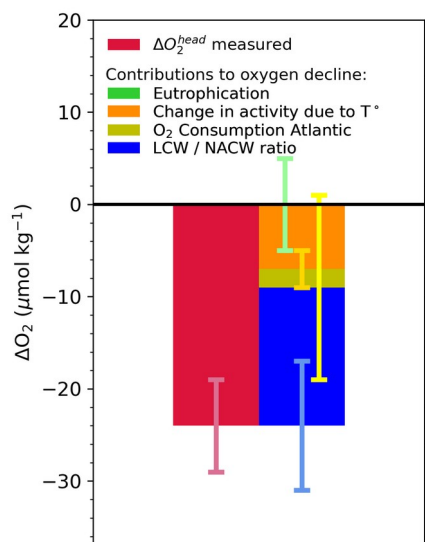


**Figure 7: Budget of drivers of deoxygenation at the head of the LSLE, from 2018 to 2021. Green: eutrophication within the Laurentian Channel; Orange: increased oxygen consumption within the channel under increased water temperature; Yellow: change in oxygen consumption in the North Atlantic, from the site of LCW and NACW mixing on the continental shelf or slope to Cabot Strait; Blue: modification of the LCW:NACW ratio at the entrance of the Laurentian Channel. See Jutras et al. (2020b) for details on the method of evaluation.**

### 3.3 Sources of water

As indicated above, water entering the Laurentian Channel (Figure 1) at depth is a mixture of two parent water masses: the relatively cold, fresher and oxygen-rich Labrador Current Water (LCW) that flows south along the western continental shelf edge of the Labrador Sea and then westward around the Grand Banks of Newfoundland, and the relatively warm, salty and oxygen-poor water of the North Atlantic Central Water (NACW) carried by the Gulf Stream (Gilbert, 2005; Jutras, 2020b). Hence, if the proportion of Labrador Current water in the mixture feeding the bottom waters of the Laurentian Channel decreases, their temperature and salinity rise, and dissolved oxygen concentrations fall.

Using a T-S diagram, Gilbert et al. (2005) estimated that, in the bottom waters of the LSLE, the proportion of LCW decreased from 72% in the 1930s to 53% in the mid-1980s, so that the proportion of NCAW or Gulf Stream water concomitantly increased from 28% to 47%. Jutras et al. (2020b) corroborated and extended these results to 2018 using an eOMP analysis, and estimated that the proportion of LCW decreased from ~60% in the 1970s to ~40% in 1997 and ~20% in 2018. Jutras et al. (2020b) also showed that the leading cause of bottom-water oxygen depletion in the Laurentian Channel has varied since the 1970s. Whereas eutrophication was identified as the main driver of deoxygenation at the head of the LSLE between the 1970s and early 2000s, a decrease in the relative contribution of the LCW to the bottom waters of the Laurentian Channel was the main culprit for the period between 2008 and 2018. An extension of the eOMP analysis to include the most recent data set collected in 2020 and 2021 reveals that the proportion of LCW entering the Laurentian Channel is now null, within the uncertainty (5%) of the analysis (Figure 6). In other words, North-central Atlantic waters carried by the Gulf Stream now compose nearly 100% of the waters entering the Laurentian Channel. This water has lower oxygen concentrations and is warmer, and its increased contribution explains more than 60% (~15  $\mu\text{M}$ ) of the deoxygenation (Figure 7) as well as the higher temperatures observed between 2018 and 2021. Note that this analysis only considers the



190 warming due to a change in the mixing ratio, and does not consider temperatures increases in the parent water masses themselves. Another 30% of the 2018 to 2021 deoxygenation is attributed to the increased biological oxygen consumption rates during the transit of waters along the Laurentian Channel in response to the temperature increase (Figure 7). The remaining 10% is due to a reduction of the oxygen content of the NACW, also likely due to higher water temperatures. In other words, the recent and sudden drop in bottom-water oxygen concentrations recorded since 2018 in the LSLE and GSL is entirely due to changes of the circulation patterns in the western North Atlantic, which affects dissolved oxygen both directly and indirectly, through the increase of water temperature.

### 3.4 Extent of hypoxia

195 The progressive decline of bottom-water oxygen concentrations, including the most recent drastic decrease, is not only expressed in terms of a reduction in minimum dissolved oxygen values, but also as an expansion of the hypoxic zone. Whereas it was estimated that the hypoxic zone covered 1300 km<sup>2</sup> in 2003 (Gilbert et al., 2005), it reached 9400 km<sup>2</sup> in 2021 (Figures 2 and 8). The areal extent of the hypoxic zone has varied throughout the historical record, from a relatively stable 1300-2000 km<sup>2</sup> from 1995 to 2006, to 5000 km<sup>2</sup> in 2008-2011, concomitant with a decrease in the relative proportion of 200 LCW entering the Laurentian Channel and increased organic matter remineralization (Jutras et al., 2020b; Gilbert et al., 2005). The hypoxic zone then retreated to between 1000 and 2000 km<sup>2</sup> over the subsequent four years (2011-2015), before spreading to over 8000 km<sup>2</sup> in 2016. Contributing to this expansion, the area included within the 275 m isobath increases suddenly when the hypoxic zone reaches the Gulf of St Lawrence, where the Laurentian Channel widens. Notably, the five most spatially extensive hypoxic zones of the time series were recorded in the last 5 years. Severely hypoxic waters are now 205 also found at the end of the two deep channels that branch out from the Laurentian Channel, namely the Esquiman and Anticosti Channels (see years 2009 and 2021 in Figure 2).

In addition to the increasing spatial extent of the hypoxic zone, the thickness of the hypoxic layer is also increasing (Figure 3). Whereas the first observations of hypoxic waters were constrained to the bottom of the water column, at ~300 m (along the 27.25 sigma-tee isopycnal), the hypoxic layer now reaches deeper (as it expands spatially to deeper sections of the 210 Laurentian Channel) and shallower (up to 200 m, Figure 3).

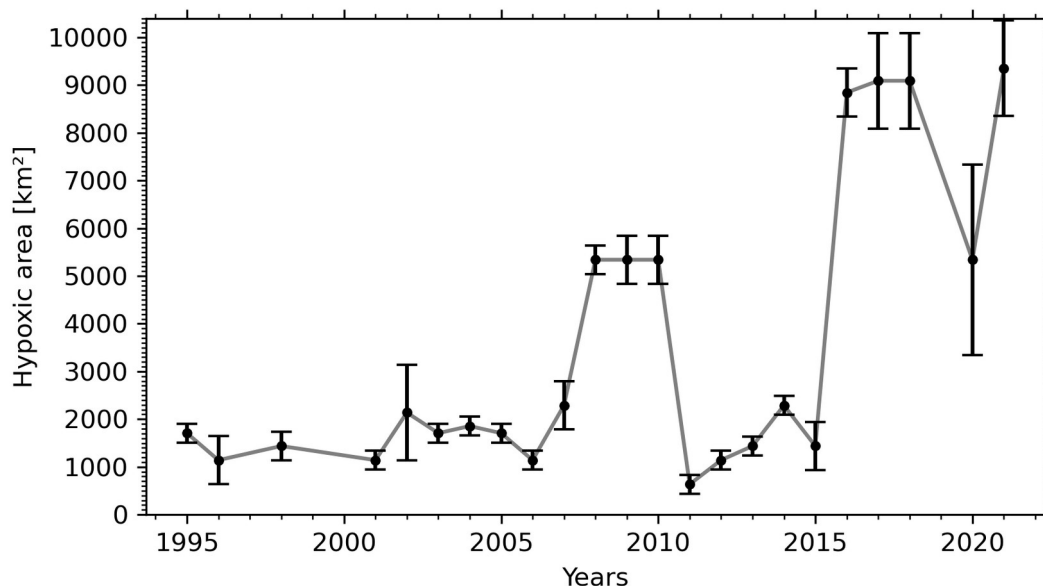


**Figure 8: Temporal variation of the areal extent of the hypoxic zone in the Laurentian Channel.**

#### 4 Conclusions

Recent observations revealed that minimum dissolved oxygen concentrations in the deep waters of the Lower St. Lawrence Estuary (LSLE) have reached unprecedented low values, dropping drastically in one year, from  $\sim 60\mu\text{M}$  or  $\sim 17\%$  saturation in 2019 to  $\sim 35\mu\text{M}$  or  $\sim 10\%$  in 2020. Concomitant with this decrease in dissolved oxygen concentrations, bottom-water temperatures have increased steadily. Like for most of the historical record of the region, the deoxygenation is driven by a change in the circulation pattern in the western North Atlantic and in the relative contribution of the parent water masses (LCW and NACW), that mix on the continental shelf or slope, and flow along the axis of the Laurentian Channel. Based on a multi-parameter water mass analysis, we have determined that the contribution of the LCW to the mixture is now nearly null.

Since the presence of hypoxic bottom water in the LSLE was first reported in 2003, the areal extent of the hypoxic zone has increased from an estimated  $1300\text{ km}^2$  to more than  $9400\text{ km}^2$  in 2021, and now extends well into the western Gulf of St. Lawrence near the tip of the Gaspé Peninsula. In some years, patches of hypoxic bottom waters can also now be found at the tip of the Anticosti and Esquiman Channels where, however, historical data coverage is limited.

#### Data Availability Statement

The two main data sets for this research are the BioChem database compiled by the Department of Fisheries and Oceans Canada as well as data collected from the RV Coriolis (spring and summer) and CCGS Amundsen (winter) data set compiled by Alfonso Mucci's research group. The BioChem database can be accessed at <https://www.dfo-mpo.gc.ca/science/data->



230 [donnees/biochem/index-eng.html](https://doi.org/10.5194/egusphere-2022-1090) and the RV Coriolis and CCGS Amundsen data sets can be accessed at on the Open Science Framework data repository at [osf.io/576tj/](https://osf.io/576tj/) and cited using the following DOI: 10.17605/OSF.IO/576TJ. For 2021, we also include data collected during the MEOPAR TReX program and the OXY21 program. These data have been collected recently and are currently not publicly available.

### Author contribution

235 AM contributed to the conceptualization, funding, and writing. DW, AM, WN, MJ and GC contributed to the data acquisition, and DW, AM and GC to their curation, including providing the required resources. MJ contributed to the analysis, visualization and writing.

### Acknowledgments

240 This study was funded by a Regroupement Stratégique grant from the Fonds de Recherche du Québec – Nature et Technologies (FRQNT) to GEOTOP, by the Natural Sciences and Engineering Research Council of Canada (NSERC) through Discovery grants to A. Mucci, G. Chaillou and D. Wallace, as well as support from MEOPAR and Réseau Québec maritime to D. Wallace for TReX (Tracer Release Experiment). M. Jutras acknowledges NSERC, the FQRNT, and Ouranos for financial support in the form of scholarships. We would like to acknowledge the help of the many students and technicians who helped in sampling and the analysis of dissolved oxygen samples throughout the years, namely Alexandre  
245 Hérard, Joannie Cool and Constance Guignard.

### References

- Audet, T., de Vernal, A., Mucci, A., Seidenkrantz, M.-S., Hillaire-Marcel, C., Carnero-Bravo, V., and Gélinas, Y. (2022) Benthic foraminifer assemblages from the Laurentian Channel in the Lower Estuary and Gulf of St. Lawrence, eastern Canada: tracers of bottom water hypoxia. *Journal of Foraminiferal Research* (submitted)
- 250 Belley R., Archambault P., Sundby B., Gilbert F., and Gagnon J.-M. (2010) Effects of hypoxia on benthic macrofauna and bioturbation in the Estuary and Gulf of St. Lawrence, Canada. *Continental Shelf Research*, 30:1302-1313.
- 255 Bindoff, N. L., Cheung, W. W., Kairo, J. G., Arístegui, J., Guinder, V. A., Hallberg, R., ... & Williamson, P. (2019). Changing ocean, marine ecosystems, and dependent communities. *IPCC special report on the ocean and cryosphere in a changing climate*, 477-587.
- Breitburg, D., Levin, L. A., Oschlies, A., Grégoire, M., Chavez, F. P., Conley, D. J., ... and Zhang, J. (2018). Declining oxygen in the global ocean and coastal waters. *Science*, 359(6371), eaam7240.
- 260 Brown-Vuillemin, S., Chabot, D., Nozères, C., Tremblay, R., Sirois, P., and Robert, D. (2022) Diet composition of redfish (*Sebastes* sp.) during periods of population collapse and massive resurgence in the Gulf of St. Lawrence. *Front. Mar. Sci.* 9:963039. doi: 10.3389/fmars.2022.963039
- 265 Bugden, G. L. (1991). Changes in the temperature-salinity characteristics of the deeper waters of the Gulf of St. Lawrence over the past several decades. *The Gulf of St. Lawrence: Small Ocean or Big Estuary*, 113, 139–147.



- 270 Chabot, D., and Claireaux, G. (2008). Environmental hypoxia as a metabolic constraint on fish: the case of Atlantic cod, *Gadus morhua*. *Marine Pollution Bulletin*, 57(6-12), 287-294.
- Chabot D., and Dutil J. D. (1999). Reduced growth of Atlantic cod in non-lethal hypoxic conditions. *Journal of Fish Biology* 55(3): 472–491. <https://doi.org/10.1006/jfbi.1999.1005>
- 275 Cyr, F., Bourgault, D., Galbraith, P. S., & Gosselin, M. (2015). Turbulent nitrate fluxes in the Lower St. Lawrence Estuary, Canada. *Journal of Geophysical Research: Oceans*, 120(3), 2308-2330.
- D'Amours, D. (1993). The distribution of cod (*Qadus morhua*) in relation to temperature and oxygen level in the Gulf of St. Lawrence. *Fisheries Oceanography*, 2(1): 24–29. <https://doi.org/10.1111/j.1365-2419.1993.tb00009.x>
- 280 Devine, L., Kennedy, M. K., St Pierre, I., Lafleur, C., Ouellet, M., and Bond, S. (2014). BioChem: The Fisheries and oceans Canada Database for Biological and chemical data (Technical Report): Fisheries and Oceans Canada.
- DFO. (2019). BioChem: Database of biological and chemical oceanographic data. Retrieved from <http://www.dfo-mpo.gc.ca/science/data-donnees/biochem/index-eng.html>
- 285 [Dickie, L., and Trites, R. \(1983\). The Gulf of St. Lawrence, In B. Ketchum \(Ed.\) Ecosystems of the World: Estuaries and enclosed seas, pp. 403–425. New York, NY: Elsevier.](#)
- 290 Dupont-Prinet, A., Pillet, M., Chabot, D., Hansen, T., Tremblay, R., and Audet, C. (2013). Northern shrimp (*Pandalus borealis*) oxygen consumption and metabolic enzyme activities are severely constrained by hypoxia in the Estuary and Gulf of St. Lawrence. *Journal of Experimental Marine Biology and Ecology* 448: 298–307. <https://doi.org/10.1016/j.jembe.2013.07.019>
- 295 Environment and Climate Change Canada (2018). *Canadian environmental sustainability indicators: Nutrients in the St. Lawrence River*. Retrieved from [www.canada.ca/en/environment-climate-change/services/environmental-indicators/nutrients-st-lawrence-river.html](http://www.canada.ca/en/environment-climate-change/services/environmental-indicators/nutrients-st-lawrence-river.html) (e2020). doi: 10.1038/ngeo2002
- 300 Galbraith, P. S. (2006). Winter water masses in the Gulf of St. Lawrence. *Journal of Geophysical Research*, 111(6). doi: 10.1029/2005JC003159
- Genovesi, L., de Vernal, A., Thibodeau, B., Hillaire-Marcel, C., Mucci A., and Gilbert, D. (2011). Recent changes in bottom water oxygenation and temperature in the Gulf of St. Lawrence: Micropaleontological and geochemical evidence. *Limnology and Oceanography* 56(4): 1319–1329. <https://doi.org/10.4319/lo.2011.56.4.1319>
- 305 Gilbert, D., Rabalais, N. N., Diaz, R. J., and Zhang, J. (2010). Evidence for greater oxygen decline rates in the coastal ocean than in the open ocean. *Biogeosciences*, 7(7), 2283-2296.
- 310 Gilbert, D. (2004). Propagation of temperature signals along the northwest Atlantic continental shelf edge and into the Laurentian Channel. Abstract, ICES CIEM Annual Science Conference, September 2004, pp. 22–25.
- Gilbert, D., Sundby, B., Gobeil, C., Mucci, A., and Tremblay, G.-H. (2005). A seventy-two-year record of diminishing deep-water oxygen in the St. Lawrence Estuary: The Northwest Atlantic connection. *Limnology and Oceanography* 50(5): 1654–1666.
- 315 Goyette, J.-O., Bennett, E. M., Howarth, R. W., and Maranger, R. (2016). Changes in anthropogenic nitrogen and phosphorus inputs to the St. Lawrence sub-basin over 110 years and impacts on riverine export. *Global Biogeochemical Cycles* 30: 1000–1014. <https://doi.org/10.1002/2016GB005384>





- 320 Grasshoff, K., Kremling, K., and Ehrhardt, M. (Eds.): *Methods of Seawater Analysis* 3rd Edn., Wiley-VCH, Weinheim, Germany, 1999.
- 325 Hudon C., Gagnon P., Rondeau M., Hebert S., Gilbert D., Hill B., Patoine M. and Starr M. (2017). Hydrological and biological processes modulate carbon, nitrogen and phosphorus flux from the St. Lawrence River to its estuary (Quebec, Canada). *Biogeochemistry* 135(3): 251–276.
- Ingram, R. (1983). Vertical mixing at the head of the Laurentian Channel, *Estuarine, Coastal and Shelf Science*, 16(3), 333-338.
- 330 Jutras, M., Mucci, A., Sundby, B., Gratton, Y., and Katsev, S. (2020a). Nutrient cycling in the Lower St. Lawrence Estuary: Response to environmental perturbations. *Estuarine, Coastal and Shelf Science* 239: 106715.
- Jutras, M., Dufour, C. O., Mucci, A., Cyr, F., and Gilbert, D. (2020b). Temporal changes in the causes of the observed oxygen decline in the St. Lawrence Estuary. *Journal of Geophysical Research: Oceans*, 125(12), e2020JC016577.
- 335 Karstensen, J., and Tomczak, M. (1998). Age determination of mixed water masses using CFC and oxygen data. *Journal of Geophysical Research: Oceans*, 103(C9), 18599-18609.
- Katsev, S., Chaillou, G., Sundby, B., and Mucci, A. (2007) Impact of progressive oxygen depletion on sediment diagenesis and fluxes: A model for the Lower St. Lawrence Estuary. *Limnol. Oceanogr.* **52(6)**: 2555-2568.
- 340 Lefort, S., Mucci, A., and Sundby, B. (2012) Sediment response to 25 years of persistent hypoxia. *Aquat. Geochem.* **18**: 461-474. doi:10.1007/s10498-012-9173-4.
- Levin, L.A. (2003) Oxygen minimum zone benthos: adaptation and community response to hypoxia. In: *Oceanography and Marine Biology: an Annual Review*, eds. Gibson, R.N. and Atkinson, R.J.A., Taylor & Francis, 41, 1-45.
- 345 Li, D.J., Zhang, J., Huang, D.J., Wu, Y., and Liang J. (2002) Oxygen depletion off the Changjiang (Yangtze River) Estuary. *Science in China. Series D: Earth Sciences* 45 (12): 1137–1146.
- 350 Mitchell, M. R., Harrison, G., Paule, K., Gagne, A., Maillet, G., and Strain, P. (2002). Atlantic zonal Monitoring Program sampling protocol. Canadian Technical Report of Hydrography and Ocean Sciences, 223 Retrieved from ISSN0711-6764.
- 355 Petersen, L. H., and Gamperl, A. K. (2010). Effect of acute and chronic hypoxia on the swimming performance, metabolic capacity and cardiac function of Atlantic cod (*Gadus morhua*). *Journal of Experimental Biology*, 213(5), 808-819.
- Rabalais, N. N., Diaz, R. J., Levin, L. A., Turner, R. E., Gilbert, D., and Zhang, J. (2010). Dynamics and distribution of natural and human-caused hypoxia. *Biogeosciences*, 7(2), 585-619.
- 360 Riedel, G.F., Sanders, J.G., and Osman, R.W. (1997) Biogeochemical control on the flux of trace elements from estuarine sediments: water column oxygen concentrations and benthic infauna. *Estuarine, Coastal and Shelf Res.* 44, 23-38.
- Riedel, G.F., Sanders, J.G., and Osman, R.W. (1999) Biogeochemical control on the flux of elements from estuarine sediments: effects of seasonal and short-term hypoxia. *Mar. Environ. Res.* 47, 349-372.
- 365 Saucier, F. J., and Chassé, J. (2000). Tidal circulation and buoyancy effects in the St. Lawrence Estuary. *Atmosphere-Ocean*, 38(4), 505-556.



- 370 Thibodeau B., de Vernal A., and Mucci, A. (2006). Recent eutrophication and consequent hypoxia in the bottom waters of  
the Lower St. Lawrence Estuary: Micropaleontological and geochemical evidence. *Marine Geology* 231(1–4): 37–50.  
[https://doi.org/10.1016/j.  
Margeo.2006.05.010](https://doi.org/10.1016/j.Margeo.2006.05.010)
- 375 Tomczak, M., and Large, D. G. (1989). Optimum multiparameter analysis of mixing in the thermocline of the eastern Indian  
Ocean. *Journal of Geophysical Research: Oceans*, 94(C11), 16141-16149.
- Tomczak Jr, M. (1981). A multi-parameter extension of temperature/salinity diagram techniques for the analysis of non-  
isopycnal mixing. *Progress in Oceanography*, 10(3), 147-171.

380